PERGAMON

International Journal of Solids and Structures 38 (2001) 4839–4855

INTERNATIONAL JOURNAL OF SOLIDS and STRUCTURES

www.elsevier.com/locate/ijsolstr

# Postbuckling behaviour of thin-walled girders with orthotropy varying widthwise

Tomasz Kubiak *

*Department of Strength of Materials and Structures (K12), Technical University of Lodz, ul. Stefanowskiego 1/15, 90-924 Lodz, PL, Poland*

Received 10 December 1999

**Abstract**

Postbuckling behaviour of elastic thin-walled orthotropic girders has been analysed within the second order of the Koiter's asymptotic stability theory of conservative systems (Koiter, 1963). Girders built of orthotropic plates with the principal directions of orthotropy parallel to the wall edges characterised by a widthwise varying orthotropy coefficient $\beta_i = E_{yi}/E_{xi}$ have been investigated. The girders with square and trapezoid sections, simply supported on the loaded edges, have been analysed. The girders have been subjected to the loads that cause a uniform and linearly variable shortening of the edges. © 2001 Elsevier Science Ltd. All rights reserved.

## 1. Introduction

Elastic buckling of isotropic and orthotropic plates and girders has been discussed in many works (e.g. Chandra and Raju, 1973; Kołakowski, 1993; Królak, 1990; Królak, 1995a and Kołakowski and Królak, 1995b). Results of these investigations show a possibility of building thin-walled structures that are light, safe and reliable.

As far as composite materials are concerned, their material properties can be freely modelled in selected directions or regions. Thus, it is possible to manufacture plates or girders with variable strength properties. Fibrous composites with properly distributed (concentrated or rarefied) fibres are examples of materials characterised by such properties. Composite materials are most often modelled as orthotropic materials. In the wide literature devoted to stability problems there is a lack of analysis of an influence of plate widthwise varying orthotropy on values of critical loads of girders built of such plates, on their modes of buckling and on postbuckling equilibrium paths of these girders.

In the present paper a problem of stability loss in an elastic range and behaviour in a postbuckling range of beam-columns with square and trapezoid sections, built of homogeneous orthotropic plates with widthwise varying orthotropy, is discussed.

* Fax: +48-42-6312217.
*E-mail address:* tomek@orion.p.lodz.pl (T. Kubiak).

0020-7683/01/$ - see front matter 
PII: S0020-7683(00)00340-1

**Nomenclature**

$a_0$, $a_1$, $a_{111}$, $a_{1111}$ coefficients of the non-linear equilibrium equation
$\overline{a}_i$, $\overline{b}_i$, $\overline{c}_i$, $\overline{d}_i$, $\overline{e}_i$, $\overline{f}_i$, $\overline{g}_i$, $\overline{h}_i$ orthogonal functions for the first order approximation fields
$\hat{a}_i$, $\hat{b}_i$, $\hat{c}_i$, $\hat{d}_i$, $\hat{e}_i$, $\hat{f}_i$, $\hat{g}_i$, $\hat{h}_i$ orthogonal functions for the second order approximation fields
$b_{1111} = a_{1111}/a_1$ postbuckling coefficient of the equilibrium equation
$b_i$ $i$th bandwidth
$D_i$, $D_{1i}$ plate stiffness of the $i$th band ($D_i = E_i \mathrm{h}_i^3/[12(1-\eta_i v_i^2)]$, $D_{1i} = G_i h_i^3/6$)
$E_i = E_{ix}$ lengthwise Young's modulus for the $i$th band of the girder wall
$E_{iy}$ widthwise Young's modulus for the $i$th band
$F_{\mathrm{cr}}$ compressive critical force corresponding to local or global buckling (N)
$G_i$ modulus of elasticity (Kirchhoff's modulus) for the $i$th band
$h_i$ thickness of the $i$th band
$i$ number of the band, wall (subscript $i = 1, 2, \ldots$)
$l$ girder length
$m$ number of halfwaves of the buckling mode in the longitudinal direction
$M_{\mathrm{cr}}$ critical moment corresponding to local or global buckling (Nm)
$M_{ix}$, $M_{iy}$, $M_{ixy}$ sectional bending moment of the $i$th band
$\overline{\mathbf{N}}$ force field
$\overline{N}_i^{(0)}$ force field of the zero state (prebuckling state)
$\overline{N}_i^{(1)}$ force field of the first order approximation (critical state)
$\overline{N}_i^{(2)}$ force field of the second order approximation (postbuckling state)
$N_{ix}$, $N_{iy}$, $N_{ixy}$ sectional membrane forces for the $i$th band
$N_{ix}^{(0)}$ prebuckling lengthwise force for the $i$th band
$N_{ix}^{(1)}$, $N_{iy}^{(1)}$, $N_{ixy}^{(1)}$ critical sectional membrane forces for the $i$th band, for the first order approximation
$N_{ix}^{(2)}$, $N_{iy}^{(2)}$, $N_{ixy}^{(2)}$ postbuckling sectional membrane forces for the $i$th band, for the second order approximation
$\overline{\mathbf{U}}$ displacement field
$\overline{U}_i^{(0)}$ displacement field of the zero state (prebuckling state)
$\overline{U}_i^{(1)}$ displacement field of the first order approximation (critical state)
$\overline{U}_i^{(2)}$ displacement field of the second order approximation (postbuckling state)
$u_i$, $v_i$, $w_i$ middle surface displacement components for the $i$th band
$u_i^{(0)}$, $v_i^{(0)}$, $w_i^{(0)}$ prebuckling displacement field for the $i$th band (zero state)
$u_i^{(1)}$, $v_i^{(1)}$, $w_i^{(1)}$ critical displacement field for the $i$th band (for the first order)
$u_i^{(2)}$, $v_i^{(2)}$, $w_i^{(2)}$ postbuckling displacement field for the $i$th band (for the second order)
$x_i$, $y_i$, $z_i$ local Cartesian system of co-ordinates for the $i$th band
$\beta_i = 1/\eta_i$ inverse of the assumed coefficient of orthotropy, assumed in order to facilitate the analysis of data
$\delta$ scalar parameter of the generalised shortening
$\delta_{\mathrm{kr}}$ critical value of $\delta$ (value of the displacement corresponding to critical load)
$\varepsilon_{ix}$, $\varepsilon_{iy}$ relative strain along $x_i$, $y_i$
$\gamma_{ixy}$ non-dilatational strain angle ($\gamma_{ixy} = 2\varepsilon_{ixy}$)

| | |
|---|---|
| $\gamma$ | coefficient of postbuckling lengthwise stiffness reduction |
| $\kappa$ | parameter of the external load distribution (ratio of the displacement of the upper part of the girder with respect to the bottom part) |
| $\eta_i = \frac{E_{iy}}{E_{ix}}$ | coefficient of orthotropy of the $i$th plate (band) |
| $\lambda$ | scalar load parameter |
| $\lambda_{\mathrm{cr}}$ | critical value of $\lambda$ (critical value of buckling) |
| $v_i = v_{ixy}$ | Poisson's ratio for the $i$th band in the $x$ direction (the first subscript denotes a transverse direction, whereas the second one – a load direction) |
| $v_{iyx}$ | Poisson's ratio for the $i$th band in the $y$ direction (the first subscript denotes a transverse direction, whereas the second one – a load direction) |
| $\varphi$ | angle enclosed between the wall "$i$" and "$i+1$" |
| $\xi$ | amplitude of the linear eigenvector of buckling (normalised with the equality condition between the maximum deflection and the thickness of the first plate $h_1$) |

## 2. Problem under consideration

Girders with closed sections (Fig. 1), built of plates with widthwise varying orthotropy (Fig. 2), have been considered. The assumed model of such a plate is built of narrow longitudinal orthotropic bands

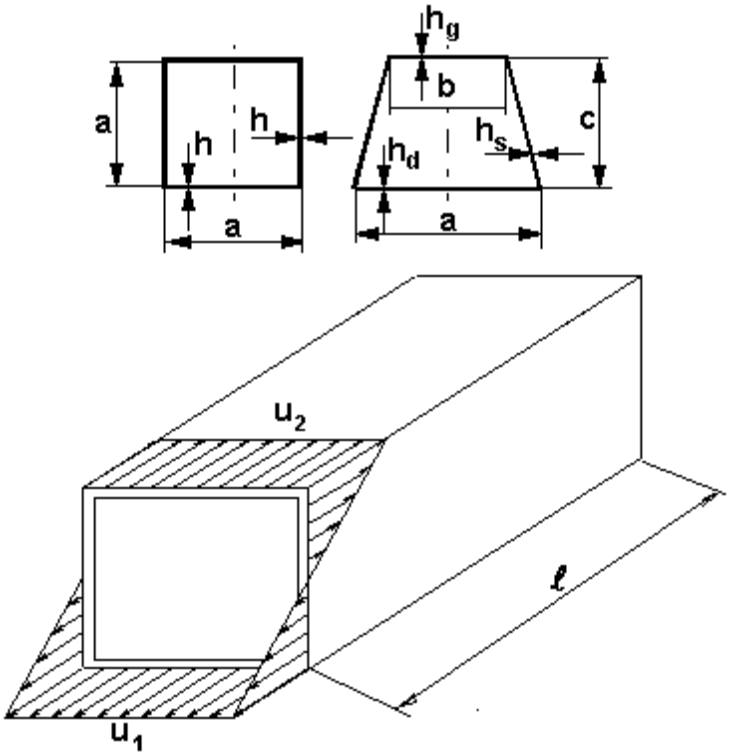


Fig. 1. Cross-sections of the girders under analysis.

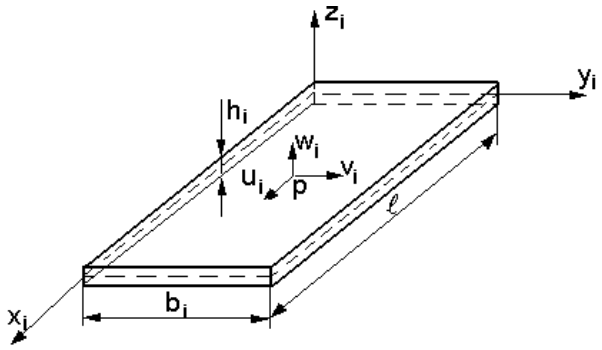


Fig. 2. Dimensions of the $i$th plate and the assumed local coordinate system.

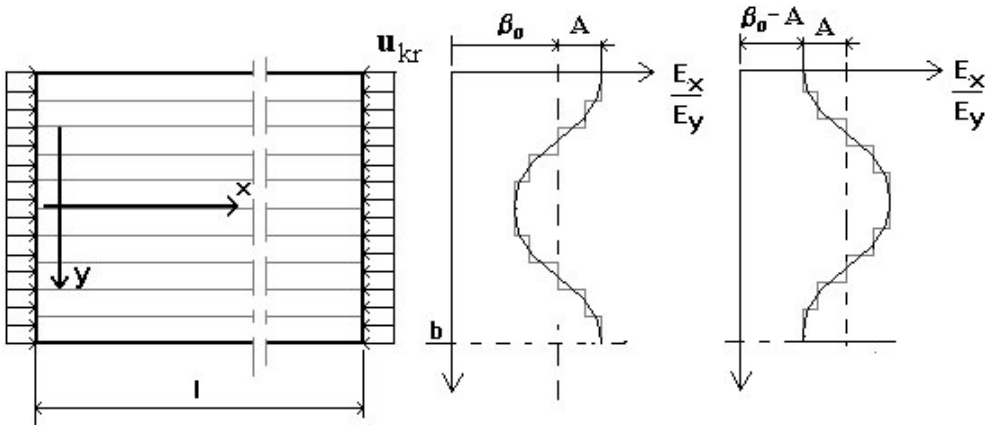


Fig. 3. Band model of a plate with variable orthotropy.

(plates), and each plate can have a different coefficient of orthotropy. The computational model describes precisely actual structural materials (Fig. 3).

A plate model has been assumed for a thin-walled beam-column. To describe the middle surface strains for each plate band, a complete strain tensor for thin plates have been assumed in the form:

$$\begin{aligned}
\varepsilon_{ix} &= u_{i,x} + \tfrac{1}{2}(w_{i,x}^2 + u_{i,x}^2 + v_{i,x}^2),\\
\varepsilon_{iy} &= v_{i,y} + \tfrac{1}{2}(w_{i,y}^2 + u_{i,y}^2 + v_{i,y}^2),\\
2\varepsilon_{ixy} &= \gamma_{ixy} = u_{i,y} + v_{i,x} + w_{i,x}w_{i,y} + u_{i,x}u_{i,y} + v_{i,x}v_{i,y},
\end{aligned} \tag{1}$$

where $u_i$, $v_i$, $w_i$-displacements parallel to the respective axes $x_i$, $y_i$, $z_i$ of the local Cartesian system of coordinates, whose plane $x_iy_i$ coincides with the middle surface of the $i$th plate ($i$th band) before its buckling (Figs. 2 and 4).

In the majority of publications devoted to structure stability problems, the terms $(u_{i,x}^2 + v_{i,x}^2)$, $(u_{i,y}^2 + v_{i,y}^2)$ and $(u_{i,x}u_{i,y} + v_{i,x}v_{i,y})$ are in general neglected for $\varepsilon_{ix}$, $\varepsilon_{iy}$, $\varepsilon_{ixy}$, correspondingly, in Eq. (1) in the strain tensor components.

Well-known relations in the theory of orthotropic plates (e.g. Chandra and Raju, 1973; Królak, 1995) describe the sectional forces and moments reduced to the middle surface of the $i$th plate ($i$th band):

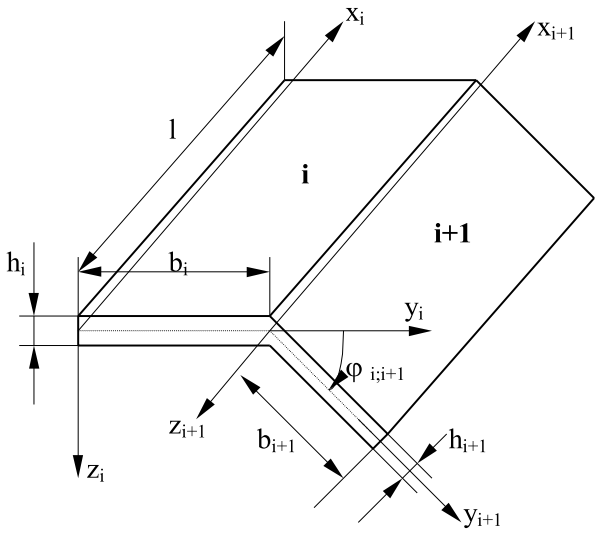


Fig. 4. Local coordinate systems of interactive plates (bands).

$$
\begin{aligned}
N_{ix} &= \frac{E_i h_i}{1-\eta_i \nu_i^2}(\varepsilon_{ix} + \eta_i \nu_i \varepsilon_{iy}),\\
N_{iy} &= \frac{E_i h_i}{1-\eta_i \nu_i^2}(\eta_i \nu_i \varepsilon_{ix} + \eta_i \varepsilon_{iy}),\\
N_{ixy} &= N_{iyx} = G_i h_i \gamma_{ixy} = 2G_i h_i \varepsilon_{ixy},\\
M_{ix} &= -D_i(w_{i,xx} + \eta_i \nu_i w_{i,yy}),\\
M_{iy} &= -\eta_i D_i(\nu_i w_{i,xx} + w_{i,yy}),\\
M_{ixy} &= -D_{1i} w_{i,xy},
\end{aligned}
\tag{2}
$$

where

$$
E_i = E_{ix}, \qquad \nu_i = \nu_{ixy}, \qquad \eta_i = \frac{E_{iy}}{E_i} \text{ – coefficient of orthotropy} \tag{3}
$$

According to the Betty–Maxwell's theorem, the Young's moduli and the Poisson's ratios occurring in Eq. (2) have to satisfy the following relation:

$$
E_{ix}\nu_{iyx} = E_{iy}\nu_{ixy}, \tag{4}
$$

and taking into account notations (3):

$$
E_i \nu_{iyx} = E_{iy}\nu_i. \tag{4a}
$$

Variational equations of equilibrium (5), kinematic and static conditions of continuity at the joints of contacting bands (8), and boundary conditions (6) on the ends under load ($x = 0$, $x = l$) follow from the principle of virtual works for a single plate band.

For an orthotropic plate in which the principal directions of orthotropy are parallel to the plate edges, the variational equations of equilibrium corresponding to Eq. (1) take the form:

$$\begin{aligned}
&\int \left( - N_{x,x} - N_{xy,y}\right)\delta u \,\mathrm{d}S = 0,\\
&\int \left( - N_{y,y} - N_{xy,x}\right)\delta v \,\mathrm{d}S = 0,\\
&\int [-\left(N_{x,x} + N_{xy,y}\right)w_{,x} - \left(N_{y,y} + N_{xy,x}\right)w_{,y} - N_x w_{,xx} - N_y w_{,yy}\\
&\qquad - 2N_{xy}w_{,xy} - M_{x,xx} - M_{y,yy} - 2M_{xy,xy}]\delta w \,\mathrm{d}S = 0
\end{aligned} \tag{5}$$

Apart from the equations of equilibrium, the following boundary conditions for $x =$ constant:

$$\begin{aligned}
&\int [N_x - \mathrm{hp}(y)]\delta u \,\mathrm{d}y = 0\\
&\int N_{xy}\,\delta v \,\mathrm{d}y = 0\\
&\int M_x\,\delta w_{,x}\,\mathrm{d}y = -\int D\left(w_{,xx} + v\eta w_{,yy}\right)\delta w_{,x}\,\mathrm{d}y = 0\\
&\int \left(N_x w_{,x} + N_{xy}w_{,y} + M_{x,x} + 2M_{xy,y}\right)\delta w \,\mathrm{d}y\\
&\quad = \int \left[N_x w_{,x} + N_{xy}w_{,y} - Dw_{,xxx} - (v\eta D + 2D_1)w_{,xyy}\right]\delta w \,\mathrm{d}y = 0
\end{aligned} \tag{6}$$

and for $y =$ constant:

$$\begin{aligned}
&\int N_{xy}\,\delta u \,\mathrm{d}x = 0\\
&\int N_y\,\delta v \,\mathrm{d}x = 0\\
&\int M_y\,\delta w_{,y}\,\mathrm{d}x = -\int \eta D\left(v w_{,xx} + w_{,yy}\right)\delta w_{,y}\,\mathrm{d}x = 0\\
&\int \left(N_y w_{,y} + N_{xy}w_{,x} + M_{y,y} + 2M_{xy,y}\right)\delta w \,\mathrm{d}x\\
&\quad = \int \left[N_y w_{,y} + N_{xy}w_{,x} - \eta D w_{,yyy} - (v\eta D + 2D_1)w_{,xxy}\right]\delta w \,\mathrm{d}x = 0
\end{aligned} \tag{7}$$

have been obtained.

The static and kinematic junction conditions on the longitudinal edges of adjacent plates, which result from Eq. (7), can be written as:

$$\begin{aligned}
&u_{i+1}|^- = u_i|^+,\\
&w_{i+1}|^- = w_i|^+\cos(\varphi) - v_i|^+\sin(\varphi),\\
&v_{i+1}|^- = w_i|^+\sin(\varphi) + v_i|^+\cos(\varphi),\\
&w_{i+1,y}\big|^- = w_{i,y}\big|^+,\\
&M_{(i+1)y}\big|^- = M_{iy}\big|^+,\\
&N_{(i+1)y}\big|^- - N_{iy}\big|^+\cos(\varphi) - Q^*_{iy}\Big|^+\sin(\varphi) = 0,\\
&Q^*_{(i+1)y}\Big|^- + N_{iy}\big|^+\sin(\varphi) - Q^*_{iy}\Big|^+\cos(\varphi) = 0,\\
&N_{(i+1)xy}\big|^- = N_{ixy}\big|^+,
\end{aligned} \tag{8}$$

where

$$\begin{aligned} M_{iy} &= -\eta_i D_i (w_{i,yy} + v_i w_{i,xx}), \\ Q^*_{iy} &= -\eta_i D_i w_{i,yyy} - (v_i \eta_i D_i + 2D_{1i}) w_{i,xxy} + N_{iy} w_{i,y} + N_{ixy} w_{i,x}, \\ \varphi &= \varphi_{i;i+1}. \end{aligned} \tag{9}$$

A non-linear stability problem has been solved by means of the Koiter's asymptotic theory (Chandra and Raju, 1973). The displacement field $\overline{U}_i$, and sectional force field $\overline{N}_i$ have been expanded into the power series with respect to the parameter $\xi$, – the buckling linear eigenvector amplitude (normalised with the equality condition between the maximum deflection and the thickness of the first plate $h_1$).

$$\begin{aligned} \overline{U}_i &= \lambda \overline{U}_i^{(0)} + \xi \overline{U}_i^{(1)} + \xi^2 \overline{U}_i^{(2)} + \cdots, \\ \overline{N}_i &= \lambda \overline{N}_i^{(0)} + \xi \overline{N}_i^{(1)} + \xi^2 \overline{N}_i^{(2)} + \cdots. \end{aligned} \tag{10}$$

By substituting expansions (10) into equations of equilibrium (5), junction conditions (8) and boundary conditions (6), the boundary problem of the zero, first and second order has been obtained (Królak, 1990, 1995). The zero approximation describes the prebuckling state, whereas the first order approximation allows for determination of critical loads and the buckling modes corresponding to them, taking into account minimisation with respect to the number of halfwaves m in the lengthwise direction. The second order approximation is reduced to a linear system of differential heterogeneous equations, whose right-hand sides depend on the force field and the first order displacements only.

Taking into account the zero, first and second order approximation, the displacements of the *i*th plate (band) have been assumed according to Eq. (10) as:

$$\begin{aligned} u_i &= \lambda u_i^{(0)} + \xi u_i^{(1)} + \xi^2 u_i^{(2)}, \\ v_i &= \lambda v_i^{(0)} + \xi v_i^{(1)} + \xi^2 v_i^{(2)}, \\ w_i &= \xi w_i^{(1)} + \xi^2 w_i^{(2)}. \end{aligned} \tag{11}$$

In the present paper, an incomplete strain tensor has been taken according to the von Kármán and Marquerre's non-linear theory of plates for a non-linear analysis of stability within the second order approximation:

$$\begin{aligned} \varepsilon_{ix} &= u_{i,x} + \tfrac{1}{2} w_{i,x}^2, \\ \varepsilon_{iy} &= v_{i,y} + \tfrac{1}{2} w_{i,y}^2, \\ 2\varepsilon_{ixy} &= \gamma_{ixy} = u_{i,y} + v_{i,x} + w_{i,x} w_{i,y}. \end{aligned} \tag{12}$$

Such an assumption has been taken after an extensive numerical analysis within the first order approximation where a complete strain tensor according to Eq. (1) and an incomplete strain tensor (12) were assumed. The most considerable differences were obtained in the values of global critical loads analysed for the second order and they did not exceed 2–3%.

The walls of the analysed girders under widthwise linearly variable load were divided into bands for which a constant value of the displacement causing a uniform shortening of edges was assumed (Fig. 5). In order to apply such a kind of load, the transition matrix method was used.

When a homogeneous zero state (prebuckling) of the *i*th plate (band) is assumed in the form:

$$\begin{aligned} u_i^{(0)} &= (l/2 - x_i) \Delta_i, \\ v_i^{(0)} &= v_i y_i \Delta_i, \end{aligned} \tag{13}$$

which, according to first expression in Eq. (2), means:

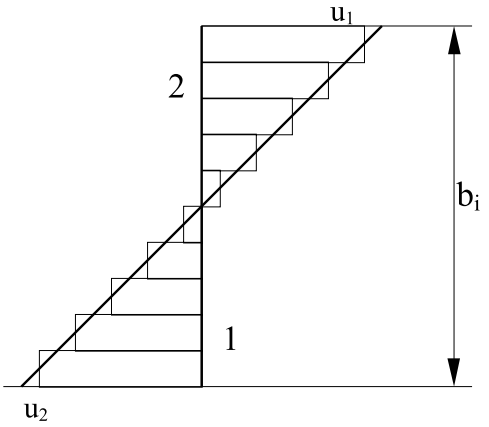


Fig. 5. Discretisation of the displacement linear distribution.

$$N_{ix}^{(0)} = -E_i h_i \Delta_i \tag{14}$$

where $N_{ix}^{(0)}$ is the current load, then the load is determined by a unit load system and by a scalar load coefficient.

Numerical aspects of convergence of the problem under consideration have decided about an introduction of the following orthogonal functions for the first order fields as boundary conditions (7) on the longitudinal edges, (for more detailed analysis see (Kołakewski, Królak, Kowal-Michalska, 1999)):

$$\begin{aligned}
&\overline{a}_i = v_{i,\chi}^{(1)} + v_i u_{i,\zeta}^{(1)}, \qquad \overline{b}_i = u_{i,\chi}^{(1)} + v_{i,\zeta}^{(1)},\\
&\overline{c}_i = u_i^{(1)}, \qquad \overline{d}_i = v_i^{(1)},\\
&\overline{e}_i = w_i^{(1)}, \qquad \overline{f}_i = w_{i,\chi}^{(1)}\\
&\overline{g}_i = w_{i,\chi\chi}^{(1)} + v_i w_{i,\zeta\zeta}^{(1)}, \qquad \overline{h}_i = E_{i2}^{*}\left(w_{i,\chi\chi}^{(1)} + v_i w_{i,\zeta\zeta}^{(1)}\right)_{,\chi} + 4w_{i,\zeta\zeta\chi}^{(1)}
\end{aligned} \tag{15}$$

where

$$\zeta_i = \frac{x_i}{b_i}, \qquad \chi_i = \frac{y_i}{b_i}.$$

In the above expressions and in the further part of this paper, the subscript "$i$" has been neglected in the derivatives with respect to $\zeta$, $\chi$.

Taking into account the relations describing the relative strains and sectional forces, as well as the orthogonal functions (15) for the first order approximation, the following system of homogeneous differential equations has been obtained:

$$\begin{cases}
\overline{a}_{i,\chi} = -\frac{1}{E_{i2}^{*}}\overline{b}_{i,\zeta},\\
\overline{b}_{i,\chi} = -E_{i1}^{*}\left(\overline{c}_{i,\zeta\zeta} + \eta_i v_i \overline{d}_{i,\zeta\chi}\right),\\
\overline{c}_{i,\chi} = \overline{b}_i - \overline{d}_{i,\zeta}\\
\overline{d}_{i,\chi} = \overline{a}_i - v_i \overline{c}_{i,\zeta},\\
\overline{e}_{i,\chi} = \overline{f}_i\\
\overline{f}_{i,\chi} = \overline{g}_i - v_i \overline{e}_{i,\zeta\zeta}\\
\overline{g}_{i,\chi} = \frac{1}{E_{i2}^{*}}\left(\overline{h}_i - 4\overline{f}_{i,\zeta\zeta}\right)\\
\overline{h}_{i,\chi} = -\frac{12 b_i^2 E_{i1}^{*}}{h_i^2}\lambda\Delta\left(1 - \eta_i v_i^2\right)\overline{e}_{i,\zeta\zeta} - E_{i1}^{*}\overline{e}_{i,\zeta\zeta\zeta\zeta} - v_i E_{i2}^{*}\overline{f}_{i,\zeta\zeta\chi}
\end{cases} \tag{16}$$

The solution to the system of equations (16) is assumed to be as follows:

$$\begin{aligned}
&\overline{a}_i = \overline{A}_i(\chi_i)\sin\frac{m\pi b_i}{l}\zeta_i, \quad \overline{b}_i = \overline{B}_i(\chi_i)\cos\frac{m\pi b_i}{l}\zeta_i, \quad \overline{c}_i = \overline{C}_i(\chi_i)\cos\frac{m\pi b_i}{l}\zeta_i, \quad \overline{d}_i = \overline{D}_i(\chi_i)\sin\frac{m\pi b_i}{l}\zeta_i,\\
&\overline{e}_i = \overline{E}_i(\chi_i)\sin\frac{m\pi b_i}{l}\zeta_i, \quad \overline{f}_i = \overline{F}_i(\chi_i)\sin\frac{m\pi b_i}{l}\zeta_i, \quad \overline{g}_i = \overline{G}_i(\chi_i)\sin\frac{m\pi b_i}{l}\zeta_i, \quad \overline{h}_i = \overline{H}_i(\chi_i)\sin\frac{m\pi b_i}{l}\zeta_i,
\end{aligned} \tag{17}$$

where $\overline{A}_i$, $\overline{B}_i$, $\overline{C}_i$, $\overline{D}_i$, $\overline{E}_i$, $\overline{F}_i$, $\overline{G}_i$, $\overline{H}_i$ are unknown functions along the transverse direction, which will be determined during numerical computations within the first order approximation by means of the transition matrix method.

Substituting the predicted solution (17) into Eq. (18), one gets the following system of ordinary differential equations:

$$\begin{aligned}
&\overline{A}_i^{\bullet} = \frac{1}{E_{i2}^*}\left(\frac{m\pi b_i}{l}\right)\overline{B}_i, \quad \overline{B}_i^{\bullet} = E_{i1}^*\left[\left(\frac{m\pi b_i}{l}\right)^2\overline{C}_i - \eta_i v_i\left(\frac{m\pi b_i}{l}\right)\overline{D}_i^{\bullet}\right], \quad \overline{C}_i^{\bullet} = \overline{B}_i - \left(\frac{m\pi b_i}{l}\right)\overline{D}_i,\\
&\overline{D}_i^{\bullet} = \overline{A}_i + v_i\left(\frac{m\pi b_i}{l}\right)\overline{C}_i, \quad \overline{E}_i^{\bullet} = \overline{F}_i, \quad \overline{F}_i^{\bullet} = \overline{G}_i + v_i\left(\frac{m\pi b_i}{l}\right)^2\overline{E}_i, \quad \overline{G}_i^{\bullet} = \frac{1}{E_{i2}^*}\left[\overline{H}_i + 4\left(\frac{m\pi b_i}{l}\right)^2\overline{F}_i\right],\\
&\overline{H}_i^{\bullet} = \left(\frac{m\pi b_i}{l}\right)^2\left[\frac{12b^2E_{i1}^*}{h^2}\lambda\Delta\left(1-\eta_i v_i^2\right) - E_{i1}^*\left(\frac{m\pi b_i}{l}\right)^2\right]\overline{E}_i + v_i E_{i2}^*\left(\frac{m\pi b_i}{l}\right)^2\overline{F}_i^{\bullet}.
\end{aligned} \tag{18}$$

In the above relations a dot (superscript) denotes a derivative with respect to $\chi_i$.

For the second order approximation, analogously as for the first order approximation, the following orthogonal functions for fields of forces and displacements have been introduced:

$$\begin{aligned}
&\hat{a}_i = v_{i,\chi}^{(2)} + v_i u_{i,\zeta}^{(2)}, \quad \hat{b}_i = u_{i,\chi}^{(2)} + v_{i,\zeta}^{(2)}, \quad \hat{c}_i = u_i^{(2)}, \quad \hat{d}_i = v_i^{(2)}, \quad \hat{e}_i = w_i^{(2)}, \quad \hat{f}_i = w_{i,\chi}^{(2)},\\
&\hat{g}_i = w_{i,\chi\chi}^{(2)} + v_i w_{i,\zeta\zeta}^{(2)}, \quad \hat{h}_i = E_2^*\left(w_{i,\chi\chi\chi}^{(2)} + v_i w_{i,\zeta\zeta\chi}^{(2)}\right) + 4w_{i,\zeta\zeta\chi}^{(2)}.
\end{aligned} \tag{19}$$

Putting the functions (15) for the first and functions (19) for the second order approximation into the equilibrium equations, we arrive at the following linear system of differential equations for the second order approximation:

$$\begin{cases}
\hat{a}_i = \hat{d}_{i,\chi} + v_i\hat{c}_{i,\zeta},\\
\hat{b}_i = \hat{c}_{i,\chi} + \hat{d}_{i,\zeta},\\
\hat{f}_i = \hat{e}_{i,\chi},\\
\hat{g}_i = \hat{f}_{i,\chi} + v_i\hat{e}_{i,\zeta\zeta},\\
\hat{h}_i = E_{i2}^*\hat{g}_{i,\chi} + 4\hat{f}_{i,\zeta\zeta},\\
E_{i2}^*\hat{a}_{i,\chi} + \hat{b}_{i,\chi} = 0,\\
E_{i1}^*\left(\hat{c}_{i,\zeta\zeta} + \eta_i v_i\hat{d}_{i,\zeta\chi}\right) + \hat{b}_{i,\chi} + \frac{E_{i1}^*}{b_i}\left(\overline{e}_{i,\zeta}\overline{e}_{i,\zeta\zeta} + \eta_i v_i\overline{f}_i\overline{f}_{i,\zeta}\right) = 0,\\
\frac{h_i^2}{12}\left(E_{i1}^*\hat{e}_{i,\zeta\zeta\zeta\zeta} + \hat{h}_{i,\chi} + v_i E_{i2}^*\hat{f}_{i,\zeta\zeta\chi}\right) + b_i\left[\overline{b}_{i,\chi}\overline{e}_{i,\zeta} - \overline{b}_{i,\zeta}\overline{f}_i - \overline{b}_i\overline{f}_{i,\zeta}\right.\\
\quad \left. + E_{i1}^*b_i\lambda\Delta\left(1-\eta_i v_i^2\right)\overline{e}_{i,\zeta\zeta} - E_{i1}^*\left(1-\eta_i v_i^2\right)\overline{c}_{i,\zeta}\overline{e}_{i,\zeta\zeta} - E_{i2}^*v_i\overline{a}_i\overline{e}_{i,\zeta\zeta}\right] = 0
\end{cases} \tag{20}$$

A solution of the system of equations (20) for the second order approximation has been assumed in the following form:

$$
\begin{aligned}
&\hat{a}_i = \sum_n \hat{A}_{in}(\chi_i)\sin\frac{n\pi b_i}{l}\zeta_i + A_i^*, \qquad \hat{b}_i = \sum_n \hat{B}_{in}(\chi_i)\cos\frac{n\pi b_i}{l}\zeta_i,\\
&\hat{c}_i = \sum_n \hat{C}_{in}(\chi_i)\cos\frac{n\pi b_i}{l}\zeta_i + C_i^*\left(\frac{l}{2}-\zeta_i b_i\right), \qquad \hat{d}_i = \sum_n \hat{D}_{in}(\chi_i)\sin\frac{n\pi b_i}{l}\zeta_i,\\
&\hat{e}_i = \sum_n \hat{E}_{in}(\chi_i)\sin\frac{n\pi b_i}{l}\zeta_i, \qquad \hat{f}_i = \sum_n \hat{F}_{in}(\chi_i)\sin\frac{n\pi b_i}{l}\zeta_i,\\
&\hat{g}_i = \sum_n \hat{G}_{in}(\chi_i)\sin\frac{n\pi b_i}{l}\zeta_i, \qquad \hat{h}_i = \sum_n \hat{H}_{in}(\chi_i)\sin\frac{n\pi b_i}{l}\zeta_i,
\end{aligned}
\tag{21}
$$

where $\hat{A}_{in}$, $\hat{B}_{in}$, $\hat{C}_{in}$, $\hat{D}_{in}$, $\hat{E}_{in}$, $\hat{F}_{in}$, $\hat{G}_{in}$, $\hat{H}_{in}$ – unknown functions which will be determined during numerical computations within the second order approximation with the transition matrix method; $A_i^*$, $C_i^*$ – constants determined form the boundary conditions for the second order approximation.

Simplicity in satisfying the orthogonality condition is one of the main reasons why the second order approximation solution in the form of series has been chosen. It follows from the orthogonality conditions of the first and second order fields that an amplitude of just one harmonics should be possibly changed for the second order.

After the substitution of the predicted solution (21) into solution (20), the following system of ordinary differential equations has been obtained:

$$
\begin{aligned}
\hat{A}_{in}^{\bullet} &= \frac{1}{E_{i2}^*}\left(\frac{n\pi b_i}{l}\right)\hat{B}_{in} - \frac{1}{2b}E_{i1}^*\left[\overline{F}_i\overline{F}_i^{\bullet} + v_i\left(\frac{m\pi b_i}{l}\right)^2\overline{E}_i\overline{F}_i\right]\{b_n\}\\
&\quad - \frac{1}{2b}E_{i1}^*\left[-\overline{F}_i\overline{F}_i^{\bullet} + v_i\left(\frac{m\pi b_i}{l}\right)^2\overline{E}_i\overline{F}_i\right]\{d_n\} - \frac{1}{E_{i2}^* b}\left(\frac{m\pi b_i}{l}\right)^2\overline{E}_i\overline{F}_i\{d_n\},\\
\hat{B}_{in}^{\bullet} &= E_{i1}^*\left[\left(\frac{n\pi b_i}{l}\right)^2\hat{C}_{in} - \eta_i v_i\left(\frac{n\pi b_i}{l}\right)\hat{D}_{in}^{\bullet}\right] + \frac{1}{2b}E_{i1}^*\left[\left(\frac{m\pi b_i}{l}\right)^3\overline{E}_i^2 - \eta_i v_i\left(\frac{m\pi b_i}{l}\right)\overline{F}_i^2\right]\{a_n\}\\
&\quad - \frac{1}{2b}E_{i1}^*\left[\left(\frac{m\pi b_i}{l}\right)\overline{F}_i^2 + \left(\frac{m\pi b_i}{l}\right)\overline{E}_i\overline{F}_i^{\bullet}\right]\{a_n\},\\
\hat{C}_{in}^{\bullet} &= \hat{B}_{in} - \left(\frac{n\pi b_i}{l}\right)\hat{D}_{in}, \qquad \hat{D}_{in}^{\bullet} = \hat{A}_{in} + v_i\left(\frac{n\pi b_i}{l}\right)\hat{C}_{in}, \qquad \hat{E}_{in}^{\bullet} = \hat{F}_{in},\\
\hat{F}_{in}^{\bullet} &= \hat{G}_{in} + v_i\left(\frac{n\pi b_i}{l}\right)^2\hat{E}_{in}, \qquad \hat{G}_{in}^{\bullet} = \frac{1}{E_{i2}^*}\left[\hat{H}_{in} + 4\left(\frac{n\pi b_i}{l}\right)^2\hat{F}_{in}\right],\\
\hat{\mathrm{H}}_{\mathrm{in}}^{\bullet} &= v_i E_{i2}^*\left(\frac{n\pi b_i}{l}\right)^2\hat{F}_{in}^{\bullet} - E_{i1}^*\left(\frac{n\pi b_i}{l}\right)^4\hat{E}_{in} + \frac{12E_{i1}^* b_i^2}{h^2}\lambda\Delta\left(1-\eta_i v_i^2\right)\left(\frac{n\pi b_i}{l}\right)^2\hat{E}_{in}\\
&\quad + \frac{12b_i}{h^2}\left\{\frac{E_{i1}^*}{2}\left[\left(1-\eta_i v_i^2\right)\left(\frac{m\pi b_i}{l}\right)^3\overline{C}_i\overline{E}_i - \eta_i v_i\left(\frac{m\pi b_i}{l}\right)^2\overline{A}_i\overline{E}_i\right] + \frac{E_{i2}^*}{2}\overline{A}_i\overline{F}_i^{\bullet} + \left(\frac{m\pi b_i}{l}\right)\overline{B}_i\overline{F}_i\right\}\{b_n\}\\
&\quad + \frac{12b_i}{h^2}\left\{\frac{E_{i1}^*}{2}\left[-\left(1-\eta_i v_i^2\right)\left(\frac{m\pi b_i}{l}\right)^3\overline{C}_i\overline{E}_i + \eta_i v_i\left(\frac{m\pi b_i}{l}\right)^2\overline{A}_i\overline{E}_i\right] - \frac{E_{i2}^*}{2}\overline{A}_i\overline{F}_i^{\bullet} + \left(\frac{m\pi b_i}{l}\right)\overline{B}_i\overline{F}_i\right\}\{d_n\}
\end{aligned}
\tag{22}
$$

if the following is taken into account:

$$\sin\frac{2m\pi b\xi}{l}=\sum a_n\cos\frac{n\pi b\xi}{l},\qquad 1=\sum b_n\sin\frac{n\pi b\xi}{l},\qquad \cos\frac{2m\pi b\xi}{l}=\sum d_n\sin\frac{n\pi b\xi}{l},$$

where

$$\{a_n\}=\frac{2}{\pi}\left(\frac{1}{2m+n}+\frac{1}{2m-n}\right),\quad \{b_n\}=\frac{4}{\pi n},\quad \{d_n\}=\frac{2}{\pi}\left(\frac{1}{n+2m}+\frac{1}{n-2m}\right),$$

where $n=1, 3, 5, 7,\ldots$, and also according to Eq. (19) $\overline{F}_i^{\bullet}=\overline{G}_i+v_i\overline{E}_i\left(\frac{m\pi b_i}{l}\right)^2$.

Having found the solutions to the first and second order of the boundary problem, the coefficients $a_0$, $a_1$, $a_{111}$, $a_{1111}$ have been determined (Królak, 1990; 1995).

$$\begin{aligned}
a_0 &= -0.5\left(\frac{\lambda}{\lambda_{\mathrm{cr}}}\right)^2\sum_i\int N_{ix}^{(0)}\varepsilon_{ix}^{(0)}\,\mathrm{d}S_i,\\
a_1 &= -\lambda\sum_i\int N_{ix}^{(0)}(w_{i,x}^{(1)})^2\,\mathrm{d}S_i,\\
a_{111} &= \tfrac{3}{2}\sum_i\int\left[N_{ix}^{(1)}(w_{i,x}^{(1)})^2+2N_{ixy}^{(1)}w_{i,x}^{(1)}w_{i,y}^{(1)}+N_{iy}^{(1)}(w_{i,y}^{(1)})^2\right]\mathrm{d}S_i,\\
a_{1111} &= 2\sum_i\int\left[N_{ix}^{(1)}w_{i,x}^{(1)}w_{i,x}^{(2)}+N_{ixy}^{(1)}\left(w_{i,x}^{(1)}w_{i,y}^{(2)}+w_{i,y}^{(1)}w_{i,x}^{(2)}\right)+N_{iy}^{(1)}w_{i,y}^{(1)}w_{i,y}^{(2)}\right]\mathrm{d}S_i\\
&\quad+\sum_i\int\left[N_{ix}^{(2)}(w_{i,x}^{(1)})^2+2N_{ixy}^{(2)}w_{i,x}^{(1)}w_{i,y}^{(1)}+N_{iy}^{(2)}(w_{i,y}^{(1)})^2\right]\mathrm{d}S_i.
\end{aligned}\tag{23}$$

The postbuckling equilibrium path is rendered by the equation:

$$a_1\left(1-\frac{\lambda}{\lambda_{\mathrm{cr}}}\right)\xi+a_{111}\xi^2+a_{1111}\xi^3=a_1\xi^*\frac{\lambda}{\lambda_{\mathrm{cr}}}\tag{24}$$

where $\lambda_{\mathrm{cr}}$ is the value of critical load.

After the determination of the coefficient $\lambda_{\mathrm{cr}}$, the coefficient of lengthwise stiffness reduction $\gamma$ has been determined on the basis of the following equations (Królak, 1995):

$$\gamma=\frac{\mathrm{d}(\lambda/\lambda_{\mathrm{cr}})}{\mathrm{d}(\Delta/\Delta_{\mathrm{cr}})}=\left(1+\frac{a_1^2\xi}{a_0(a_{111}+2a_{1111}\xi)}\right)^{-1}.\tag{25}$$

In a special case, i.e. for the so-called ideal structure without initial imperfections ($\xi^*=0$) and when the equilibrium path ($a_{111}$) is symmetrical, the postbuckling equilibrium path is defined by the equation:

$$\frac{\lambda}{\lambda_{\mathrm{cr}}}=1+b_{1111}\xi^2\tag{26}$$

and the coefficient of lengthwise stiffness reduction is:

$$\gamma=\left(1+\frac{a_1^2}{2a_0a_{1111}}\right)^{-1}\tag{27}$$

where $b_{1111}=a_{1111}/a_1$.

The detailed numerical analysis has shown that the values of the coefficient $a_{111}$ for the cases under consideration can be disregarded in practice.

## 3. Results of calculations

Girders with closed square and trapezoid sections, characterised by the following dimensions, have been analysed (Fig. 1):

- square section: $a = 100$ mm; $h = 1$ mm (wall thickness); $L = 2750$ mm
- trapezoid section: $a = 100$ mm; $b = 50$ mm; $c = 95.476$ mm; $L = 2750$ mm; thickness of the respective walls: $h_d = 1.7$ mm; $h_g = 0.5$ mm; $h_s = 1.075$ mm

In order to characterise the way the load is applied, the coefficient of edge shortening $\kappa = u_1/u_2$ has been introduced, where $u_1$, $u_2$ are values of displacements of the upper and bottom girder plates for $x = 0$, $l$ (Fig. 1). All the beam-columns under analysis were built of plates having a geometrical and material axis of symmetry.

In order to facilitate the results of numerical analysis, the second coefficient of orthotropy $\beta = 1/\eta = E_x/E_y$ has been introduced. With the coefficient of orthotropy defined in such a way, its increase means an increase in the lengthwise stiffness $E_x$ of girder walls.

Sample results of numerical investigations are presented in the form of diagrams describing critical quantities (the force $F_{cr}$, the moment $M_{cr}$ or both the force and moment) as functions of a parameter describing orthotropy variability. The amplitude $A$ of the sinusoid depicting a change of orthotropy (Fig. 5) is such a parameter. As a result of the analysis within the second order approximation, we have obtained $b_{1111} = a_{1111}/a_1$ (coefficient describing the character of the postbuckling equilibrium path) and $\gamma$ (lengthwise stiffness reduction coefficient), which are shown on diagrams as functions of the variable $A$.

Indispensable relations between the coefficient of orthotropy and $E_i$, $E_{yi}$, $G_i$, $\nu_{xyi}$ for the sinusoidally varying coefficient of orthotropy $\beta_i$ have been obtained by an approximation (Fig. 6) of the material data (Chandra and Raju, 1973) and they assume the following form:

$$E_i = \beta_i E_{yi}, \qquad E_{yi} = 34807 - \frac{11629}{\beta_i} - \frac{16821}{\beta_i^2}, \qquad G_i = 14605 - \frac{7812}{\beta_i} - \frac{3464}{\beta_i^2}, \qquad \nu_i = 0.3 \text{ for } i = 1, \ldots, n,$$

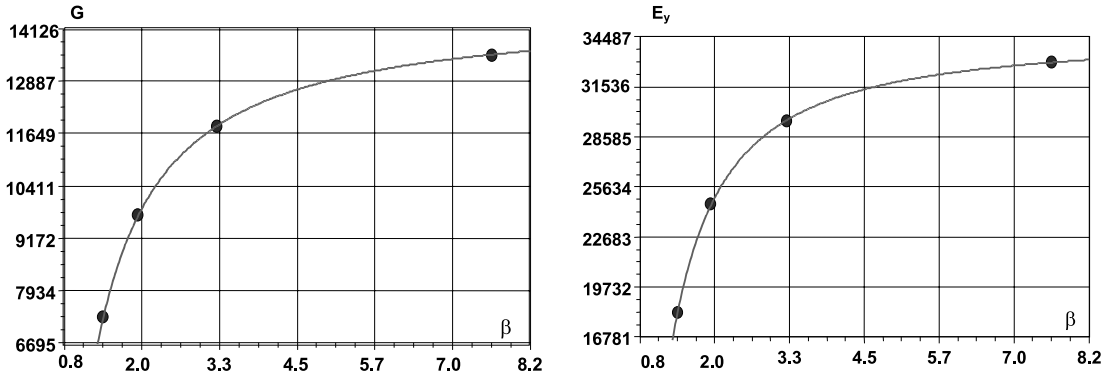


Fig. 6. Curves describing the relation of $G$ and $E_y$ as a function of the coefficient of orthotropy $\beta$ (●): points obtained on the basis of the material data taken from the literature [2], (—): curved obtained as a result of approximation.

The coefficients of orthotropy for individual bands of the model are assumed according to the formula:

$$\beta_i = \beta_0 + A\cos\frac{2\pi y_i}{b_i},$$

where $\beta_0 = 3.2292$, $A \in \langle -2,2\rangle$: sinusoid amplitude, $y_i$: coordinate defining the distance of the band from one of the longitudinal edges, $b_i$: plate width.

### 3.1. Results obtained from first order approximation

Fig. 7 presents critical quantities for the girder with a square section subjected to the load that causes a linearly variable shortening of edges ($\kappa = -1$), corresponding to pure bending. As can be seen in Fig. 7, all the curves are of an increasing character. An increase in the amplitude $A$ from $-2$ to 2 causes approximately a triple increase in the critical moment for the global symmetric mode of buckling, a 50% increase for the antisymmetric mode of global buckling and twice as large an increase in critical load for local stability loss. As it is clear that the critical values corresponding to local stability loss are many times lower than the critical values for global modes, only postcritical quantities corresponding to local buckling have been analysed.

For local stability loss, a change in the amplitude $A$ causes an insignificant change of the buckling mode, i.e. an increase in the number of halfwaves occurring during stability loss (Table – Fig. 7).

Figs. 8 and 9 present the values of critical loads for girder with a trapezoidal section, built of walls characterised by a widthwise sinusoidally variable coefficient of orthotropy. The crosswise dimensions of the trapezoid girder have been selected in such a manner that the moments of inertia with respect to the section principal axes of inertia are the same. The girder has been loaded in a way causing a uniform shortening of edges $\kappa = 1$. As the neutral axis of the section does not coincide with the material axis of symmetry, the force and moment are critical quantities under such circumstances (eccentric compression corresponds to a uniform edge shortening).

Global (Eulerian $m = 1$) and local ($m \neq 1$) flexular buckling have been analysed. The values of global symmetric and antisymmetric critical load (marked as "Global Sym" and "Global Asym", respectively – see Fig. 8) are equal in the beam model. In the case of the plate model, as can be seen in Fig. 8, a certain role is played by material asymmetry of the section, i. e. displacement of the material symmetry axis of side walls

| A | m | M[Nm] |
|---|---|---|
| -2 | 22 | 180 |
| -1 | 23 | 242 |
| 0 | 25 | 306 |
| 1 | 26 | 386 |
| 2 | 27 | 493 |

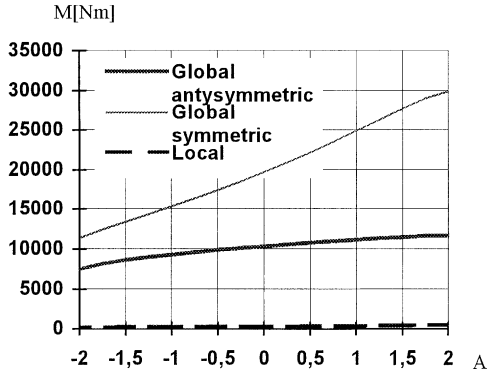


Fig. 7. Influence of the amplitude $A$ on a value of the critical moment for the girder with a square section and the coefficient of edge shortening $\kappa = -1$.

| first local mode | | | | | | second local mode | | | | | |
|---|---|---|---|---|---|---|---|---|---|---|---|
| A | -2 | -1 | 0 | 1 | 2 | A | -2 | -1 | 0 | 1 | 2 |
| m | 22 | 23 | 24 | 26 | 27 | m | 51 | 55 | 59 | 63 | 68 |
| F[kN] | 6.3 | 7.4 | 8.5 | 9.8 | 11.5 | F[kN] | 6.6 | 8.2 | 9.6 | 11.3 | 14.1 |
| M[Nm] | 43 | 51 | 58 | 67 | 78 | M[Nm] | 45 | 56 | 66 | 78 | 96 |

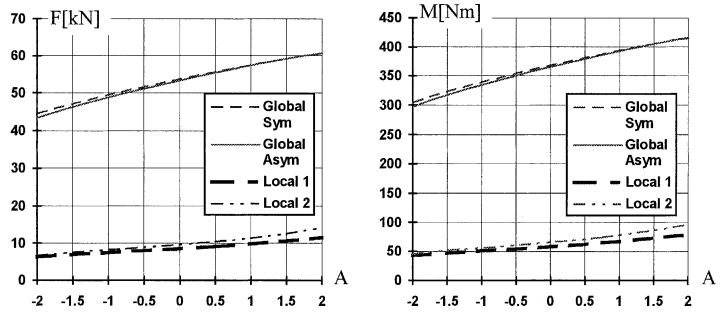


Fig. 8. Influence of the amplitude $A$ on a value of the critical force for the girder with a trapezoid section and the coefficient of edge shortening $\kappa = 1$.

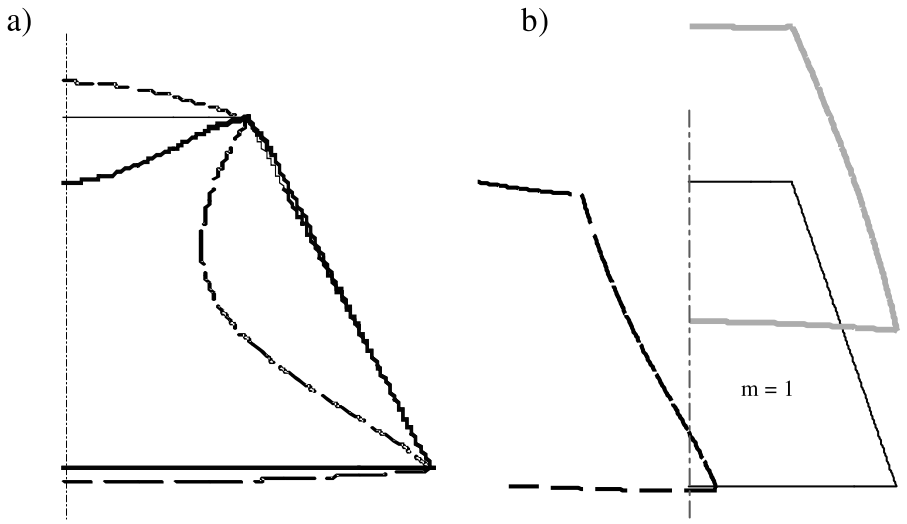


Fig. 9. Buckling modes: (a) local and (b) global.

with respect to the horizontal central axis of inertia of the section. Both the global modes are flexular in two planes perpendicular with respect to each other (Fig. 9b). Such an analysis is not possible when the beam model of the orthotropic column is assumed.

The values of local loads for two significantly different numbers of halfwaves of buckling $m$ are close, but various modes of buckling correspond to them (Fig. 9a). For the first local mode, the web loses stability at first, whereas for the second mode – it is the upper plate to lose stability first.

As can be seen in Fig. 8, all critical quantities increase with an increase in the amplitude $A$, i.e. for the girder under analysis an increase in the wall edge stiffness causes an increase in critical load that results in

stability loss. If the values are analysed, it can be seen that an increase in the critical force and moment equals to approximately 30% for global modes and it is nearly twice as large for local modes at a change in the amplitude $A$ from $-2$ to 2.

With an increase in the amplitude $A$, a mode of buckling changes as well, and the number of buckling halfwaves $m$ increases (Fig. 8 – Table).

### 3.2. Results obtained from second order approximation

Fig. 10 presents postbuckling behaviour of girder with a square section subjected to the load that causes a linearly variable shortening of edges ($\kappa = -1$), corresponding to pure bending. It shows an influence of the amplitude $A$ on a value of the coefficient of stiffness reduction $\gamma$ and the coefficient $b_{1111}$ which is a coefficient in the equation of the parabola describing the postbuckling equilibrium path (26). With an increase in the amplitude $A$, the coefficient of stiffness reduction $\gamma$ increases by approximately 60%, whereas the coefficient $b_{1111}$ increases for $A$ from $-2$ to 0 and decreases for $A$ from 0 to 2.

Figs. 11 and 12 present postbuckling behaviour of girder with a trapezoidal section, which has been loaded in a way causing an uniform shortening of edges $\kappa = 1$.

Fig. 11 presents the lengthwise stiffness reduction coefficient $\gamma$ and the coefficient $b_{1111}$ of the equation describing the postbuckling equilibrium path as a function of the amplitude $A$ of the sinusoid describing a

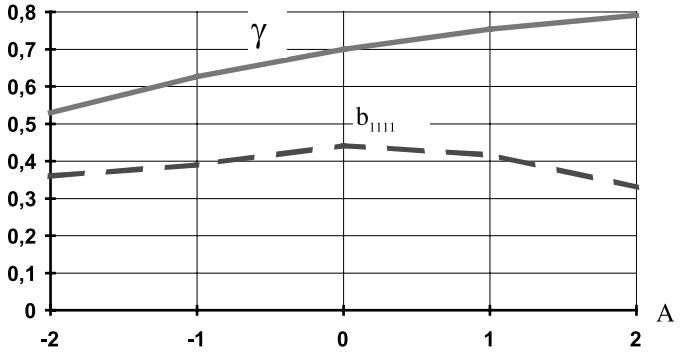


Fig. 10. Influence of the amplitude $A$ on values of the coefficients $\gamma$ and $b_{1111}$ for the girder with a square section and the coefficient of edge shortening $\kappa = -1$.

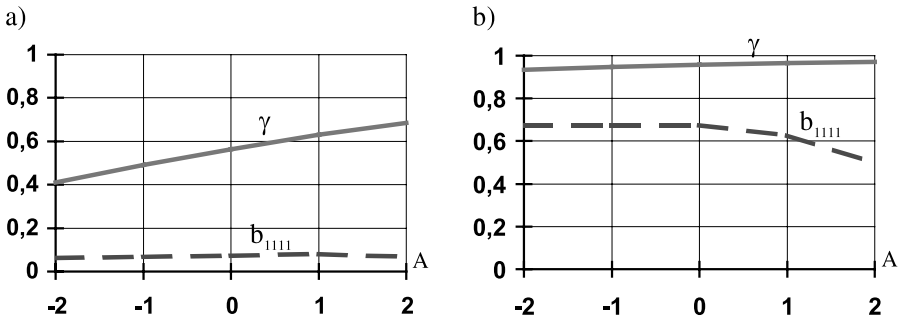


Fig. 11. Influence of the amplitude $A$ on the values of the coefficients $\gamma$ and $b_{1111}$ for the girder with a trapezoid section and the coefficient of edge shortening $\kappa = 1$: (a) first local mode, (b) second local mode.

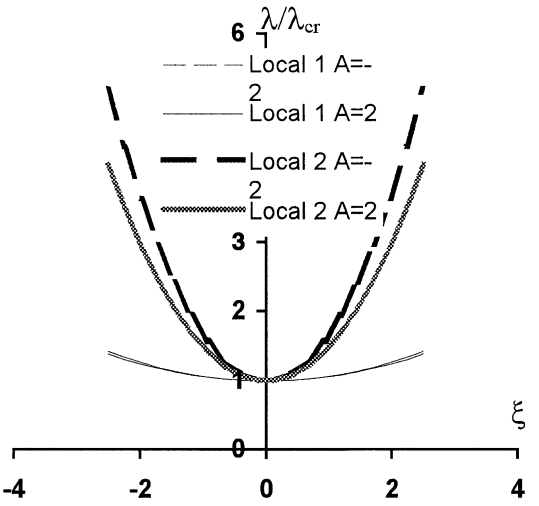


Fig. 12. Postbuckling equilibrium paths for the girder with a trapezoid section and the load coefficient $\kappa = 1$.

change in the orthotropy coefficient along the width of the girder wall. As can be seen in the diagram, reinforcement of plate edges stiffness results in an increase in the coefficient $\gamma$. On the other hand, the coefficient $b_{1111}$ increases only in the range of $A$ from $-2$ to 0 and it decreases in the range from 0 to 2.

In Fig. 12 postbuckling equilibrium paths corresponding to the first and second local buckling mode for the girder with a trapezoidal section and the coefficient of edge shortening $\kappa = 1$ for extreme values of the amplitude $A = -2$ and 2 under analysis are shown. The postbuckling equilibrium paths for the first local mode are more flat than the ones referring to the second mode. More disadvantageous postbuckling behaviour of the structure corresponds to the buckling of the first local mode.

## 4. Conclusions

A non-linear analysis of buckling for thin-walled structures with widthwise varying orthotropy has been carried out.

The numerical computation results discussed in the present paper show that for the structures under investigation a higher coefficient of orthotropy on the plate edges results in an increase in critical stresses in beam columns subject to loads causing a uniform ($\kappa = 1$) and linearly variable ($\kappa = -1$) shortening of edges. An analysis of the quantities characterising postbuckling behaviour of the structure has shown that the stiffness reduction coefficient $\gamma$ grows with an increase in the amplitude $A$, that is to say, with an increase in the stiffness of girder wall edges.

Thus, we can draw a conclusion that if a kind of load, boundary conditions and structure geometry are given, we can choose such a function describing the orthotropy variability along the wall width that the critical load of the structure reaches a required values and the postbuckling behaviour.

## Acknowledgements

The paper has been carried out within the frame of the research project no. PB 251/T07/97/12 supported by the State Committee for Scientific Research, Poland.

## Appendix A. The following notation has been used:

$$(\ldots)_{,x} = \frac{\partial(\ldots)}{\partial x}, \qquad (\ldots)_{,y} = \frac{\partial(\ldots)}{\partial y},$$

$$(\ldots)_{i,\zeta} = \frac{\partial(\ldots)}{\partial \zeta_i}, \qquad (\ldots)_{i,\chi} = \frac{\partial(\ldots)}{\partial \chi_i} = (\ldots)_i^{\bullet},$$

$$\zeta_i = \frac{x_i}{b_i}, \qquad \chi_i = \frac{y_i}{b_i},$$

$$E_{i1}^* = \frac{E_i}{G_i}\frac{1}{1-\eta_i v_i^2}, \qquad E_{i2}^* = \frac{E_i}{G_i}\frac{\eta_i}{1-\eta_i v_i^2} = \eta_i E_{i1}^*.$$

## References


Chandra, R., Raju, B., 1973. Postbuckling analysis for rectangular orthotropic plates. International Journal of Mechanics and Science 16, 81–97.

Koiter, W.T., 1963. Elastic stability and post-buckling behaviour. Proceedings of the Symposium on Nonlinear Problems. University of Wisconsin Press, Wisconsin, pp. 257–275.

Kołakowski, Z., 1993. Interactive buckling of thin-walled beam-columns with open and close cross-sections. Thin-Walled Structures 15, 159–183.

Kołakowski, Z., Królak, M., 1995a. Interactive elastic buckling of thin-walled closed orthotropic beam-columns. Engineering Transaction 4, 571–590.

Królak, M., Kołakowski, Z., 1995b. Interactive elastic buckling of thin-walled open orthotropic beam-columns. Engineering Transaction 4, 591–602.

Kołakowski, Z., Królak, M., Kowal-Michalska, K., 1999. Modal interactive buckling of thin-walled composite beam-columns regarding distortional deformations. International Journal Engineering and Science 37, 1577–1596.

Królak, M. (Ed.), 1990. Postbuckling behaviour and limit load carrying capacity of thin-walled girders with flat walls. PWN, Polish Scientific Publishers, Warszawa-Lódź, (in Polish).

Królak, M. (Ed.), 1995. Stability, post-buckling and load carrying capacity of thin-walled orthotropic structures with flat walls. Technical University of Lódź Monographs (in Polish).